CIMAC CONGRESS 25
ZURICH, MAY 19 – 23, 2025

2025 | 526

Optimizing ammonia-hydrogen combustion for high-performance marine engines: insights from experimental and CFD investigations

Fuel Injection & Gas Admission and Engine Components

Arne Güdden, FEV GmbH

Maximilian Bierl, FEV
Avnish Dhongde, FEV
Aleksandar Boberic, FEV
Stefano Ghetti, FEV
Thomas Körfer, FEV

ABSTRACT

Decarbonization is currently the driving force in the entire industrial propulsion, power generation, and energy sector, as it is essential to fulfil the environmental protection requirements concerning GHG emissions and associated global warming. However, it is unquestioned, that the future of carbon-free power generation depends above all on the utilization of renewable, low or even carbon-neutral energy carriers, that can meet the increasing energy demand while minimizing the environmental impacts of energy production and energy utilization.

The marine industry is also actively exploring the transition to sustainable fuel alternatives and carbon neutral solutions while complying at the same time with even more stringent emissions regulations. In this context, ammonia (NH3) has gained considerable attention as a promising carbon-free fuel because of its potential to reduce greenhouse gas emissions when used in converted or dedicated marine engines. As a hydrogen carrier with higher energy density, NH3 can play a crucial role in the decarbonization of shipping and maritime transport. However, NH3 is in general characterized by rather poor combustion properties, such as low combustion speed and high ignition temperature, which hinder its effective use in traditional marine engines. Recent findings indicate that engine performance can be significantly increased by mixing NH3 with hydrogen (H2) which increases the fuel conversion and the combustion speed [1,2,3].

This paper examines many facets of advanced and efficient NH3 combustion in marine engines and highlights its functionality in different combustion modes, including spark ignition (SI), pre-chamber utilization and diesel pilot injection. FEV has undertaken extensive single-cylinder engine (SCE) investigations with ammonia employing both spark ignition (SI) and diesel pilot ignition methods. These investigations have been supported by a sophisticated tool chain including advanced 3D computational fluid dynamics (CFD) models, which have been continuously calibrated on the base of fundamental research activities and additionally by the experimental results. These simulations, which were calibrated to experimental data, were then fed back and applied to a high-speed marine engine to investigate the effects of different hardware, operating parameters and calibration settings, for e.g. the variation of start of injection (SOI), lambda (air-fuel ratio), hydrogen content in the fuel blend, and the compression ratio (CR). The results demonstrate the high potential of NH3-H2 blends in stabilizing and optimizing the combustion processes and offer a viable path for the marine industry to convert to sustainable, carbon-neutral fuels in a tailored manner.

1 INTRODUCTION

In the maritime sector, for example, the European Union has taken the bold decision to integrate shipping under the Emission Trading Scheme and launch the so-called FuelEU Maritime Initiative to promote the introduction of sustainable marine fuels and zero-emission technologies [4].

Hydrogen and ammonia have been identified in this context as viable energy carriers to safeguard the timely decarbonization of the maritime and power generation sectors. Especially, H_2 has been identified in general as a prime facilitator of a fast and sustainable carbon-neutral economy. Nevertheless, the issues and challenges associated with H_2 like energy density, storage, transportation and distribution and infrastructure deployment have hindered its large-scale integration into the established energy system for the time being and in the short term. Conversely, NH_3 presents itself in this regard as an efficient carbon-free hydrogen carrier, depicted by a high energy density and a well-established, adaptable infrastructure capable of addressing several of the primary limitations of hydrogen [1,5].

In terms of its combustion properties, NH_3 faces several challenges compared to the current predominant hydrocarbon fuels. It features a comparably high ignition temperature, a rather low flame speed, a narrow flammability window, a high heat of vaporization, generally slow chemical kinetics, and, due to the fuel-bound nitrogen, combustion of ammonia is prone to formation of NO_x or N_2O [1,6]. While NO_x represents a harmful, and strictly regulated, atmospheric pollutant, N_2O is globally the third most relevant greenhouse gas after methane and CO_2 and features a nearly 300 times higher global warming potential (GWP) than CO_2 [1,7]. The inferior combustion properties of NH_3 mean that different, partially novel combustion strategies than those of hydrocarbon fuels are needed. In practice, this means that one must overcome the challenge of low reactivity of NH_3 while simultaneously mitigating the pollutant formation. Early research activities in the 1960s indicated already successful combustion of pure NH_3 in compression ignition (CI) engines, but only for extremely high compression ratios (> 35:1) and under very particular operating conditions. [1]. Latest research in the conversion of CI base engine to low carbon operation has focused more on dual-fuel strategies, where a more reactive agent is used either as a powerful ignition enabler or admixed to uplift the reactivity of the mixture. Often, these solutions still rely on fossil fuels, such as classical diesel, which produce carbon emissions during the fired engine operation. As a useful and beneficial supplement, H_2, which is highly reactive and has a low ignition energy and a high flame speed, can be considered as a carbon-free combustion enabler for NH_3. This promising option provides a further benefit by offering the potential to avoid a separate 2nd tank system on board for a second fuel, as H_2 can be produced through in situ NH_3 decomposition.

In this paper, FEVs high-speed SCE was selected for a dedicated research case study. The engine was converted from a classical diesel combustion system to a multifuel configuration, combining a DI H_2 injection with a port NH_3 fuel supply. Ignition of the premixed fuel was foreseen to be performed either with a spark plug, a pre-chamber or via pilot diesel injection emphasizing the different potential applications i.e. in stationary power generation and marine. The focus of the experiments presented in this paper lays on the investigations with spark- and pre-chamber ignition. The goal of the experimental test campaigns was mainly oriented to explore different options to convert a diesel engine to NH_3 with varying degrees of required modifications. The initial experimental tests were then used to calibrate a sophisticated 3D CFD toolchain. After calibration, an extensive simulation matrix on a large bore high-speed engine was performed to investigate ammonia combustion with supplement hydrogen ignited by diesel pilot in various shares and engine setups, of which some representative results will be presented within this publication.

2 CASE SETTING AND CONFIGURATION

For the experimental investigations, FEV's advanced high-speed diesel SCE featuring high mechanical strength, was modified to operate in various combustion configurations. Besides conventional diesel combustion, the engine was already operated on pure hydrogen and on methanol in mono- and dual-fuel mode for previous publications [8,9]. From these investigations, combustion systems with spark and prechamber ignition, but also premixed low pressure and diffusive high pressure dual fuel configurations are available. So far, the single cylinder engine was already operated in spark ignition, pre-chamber ignition and low pressure pre-mixed dual fuel combustion mode. An overview of the main characteristics of FEV's high-speed single cylinder engine is shown in Figure 1.

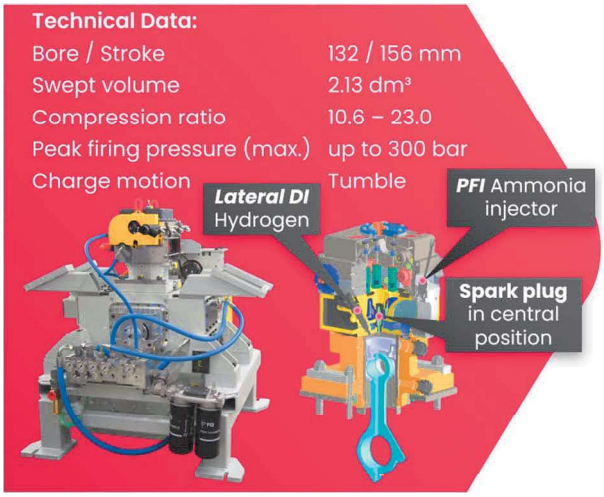

Figure 1 – Test Objective and Specification

With the focus of the presented experimental investigations being on spark and pre-chamber ignition of NH_3 and NH_3-H_2 blends, the key modifications are as follows.

A piston with a pot bowl design has been chosen to achieve a comparatively low compression ratio (CR) of 11.5:1 as well as a moderately increased one of 15:1. The lower CR is intended for H_2 blending in high shares while the higher CR is focused on pure ammonia combustion. The piston design generates a squish flow with both geometries, which in turn produces additional turbulence at the end of the compression stroke to support the combustion speed.

The cylinder head was accordingly redesigned to implement H_2 low-pressure direct injection in a lateral position. A common parts approach to the diesel base engine was applied with high carry over. For the investigations with positive ignition, despite the flat cylinder head design, the intake ports are constructively adapted – supported by FEV's charge motion design process (CMD) – with the aim to generate a moderate level of tumble motion, which has already led to excellent combustion characteristics in pure hydrogen operation resulting in the achievement of a maximum engine load of IMEP = 30 bar. Moreover, the centrally located spark plug favourably enables to implement a conventional J-Gap spark plug as well as a passive pre-chamber spark plug.

The ammonia was pre-evaporated and injected in gaseous state into the intake port. All NH_3 lines were heated and isolated to avoid condensation, see Figure 2.

For all measurements, the exhaust backpressure was controlled to be equal to the boost pressure for unthrottled operating points. To avoid severe engine damage, the operating limits of this engine have been defined by the maximum pre-ignition frequency, knock peak-to-peak (KPP) and maximum peak firing pressure (PFP) parameters respectively.

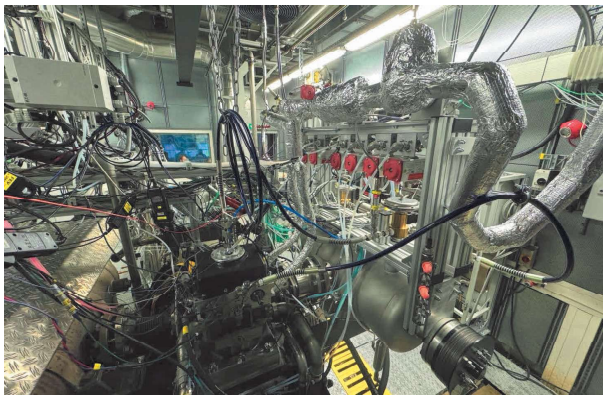

Figure 2 – Ammonia supply in the test cell

3 EXPERIMENTAL INVESTIGATIONS

This experimental section aims to provide insights to combustion of NH_3 with positive ignition. To calibrate the CFD models, positive ignition was used to distinguish the influence of diesel ignition and the NH_3 related heat release. The investigation matrix was performed with different CR settings, spark plug and passive prechamber. Moreover, varying shares of H_2 were applied to calibrate the CFD models also for potential H_2 blending. Some representative results with the calibrated CFD model can be found in Section 4 for better visualization.

3.1 VARIATION OF THE AMMONIA ENERGY SHARE

Figure 3 shows a variation of the ammonia energy fraction for different CR and with different ignition systems at a medium load point IMEP = 10.6 bar with stoichiometric air fuel ratio and fixed center of combustion (COC) at 1200 1/min.

In all cases, the indicated thermal efficiency (ITE) is significantly higher for CR = 15:1 as compared to CR = 11.5:1 since for both setups, a COC = 8° CA ATDC offers knock free engine operation. However, the hydrogen energy share is limited to approx. 20% with CR = 15:1. For higher shares, the occurrence of pre-ignition prevents stable combustion. With a CR = 11.5:1, conventional spark knock is observed at hydrogen energy fractions of approx. 50%.

While the ITE does not significantly vary with the NH_3 energy share, the coefficient of variation (COV) of IMEP rises sharply for the J-Gap spark plug with small electrode gap and for the pre-chamber spark plug at the highest NH_3 shares for

CR = 11.5:1. This delivers clear evidence of the low ignitability of ammonia that is manifesting in a prolonged burn delay. The less H_2 is mixed to the NH_3, the more difficult it is to ignite the mixture. For CR = 15:1, this tendency is not prominent due to the overall increased temperatures inside the combustion chamber.

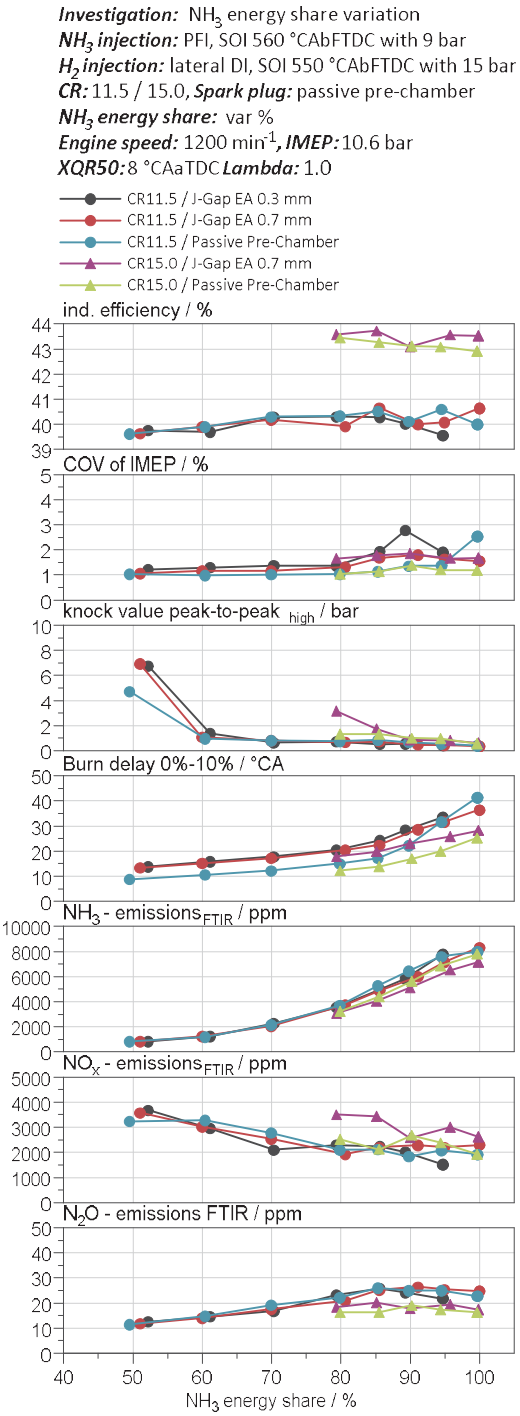

Figure 3 – Ammonia energy share variation with different ignition setups

For the investigations at comparatively low load, the NH_3 emissions are on a relatively high level with about 8000 ppm for pure ammonia operation and display a sharp decline with increasing H_2 content. There is a trend of a minor reduction of the NH_3 emissions for the higher compression ratio. This is contradictory to the typically expected trend of higher quenching effects due to more fuel being present in cavities at the high compression ratio. This again underlines the analysis that the combustion of ammonia is more severely enhanced by the higher temperatures inside the combustion chamber as known from other conventional fuels.

In comparison to the NH_3 emissions, the NO_x emissions are on a level comparable to e.g., gasoline engines operated with stoichiometric combustion and tend to decrease with increasing ammonia share. Ammonia has a rather low combustion temperature [10]. At stoichiometric combustion, the nitrogen chemistry involved in ammonia oxidation is not leading to a significant increase in the nitrogen oxide emissions. N_2O emissions on the other hand rise with increasing ammonia share. At a CR = 11.5:1 the emissions are approx. 25 ppm while they are approx. 18 ppm for CR = 15:1. This shows the tendency of ammonia oxidation is to form N_2O at low combustion temperatures. By elevating the temperature level further, N_2O formation can be accordingly reduced.

3.2 VARIATION OF THE AIR-FUEL-RATIO

Figure 4 provides an air-fuel-ratio (rel. AFR) variation at a mid torque point of IMEP = 10.6 bar and 1200 1/min. Here, the passive pre-chamber was installed for all the variations. For a CR = 11.5:1 an NH_3 energy share of 80% is depicted while for CR = 15:1 a 100% ammonia operation is shown as well.

The results provide further evidence that hydrogen blending enhances the combustion stability and speed of ammonia. For a CR = 15:1, the lean burn limit is shifted from rel. AFR = 1.3 to rel. AFR = 1.65. Moreover, improved combustion with a CR = 15:1 is observed, shifting the lean burn limit by 0.2 units of the rel. AFR compared to CR = 11.5:1 for 80% NH_3 energy share. The indicated efficiency peaks in lean operation with approximately 0.2 rel. AFR units to the lean burn limit representing a well-known behavior from other fuels.

Ammonia emissions bottom out around a rel. AFR = 1.2. Contrarily to conventional fuels, NO_x emissions continue to stay at a higher level even after rel. AFR = 1.2 because the higher oxygen availability contributes to higher fuel NO_x produced by the NH_3 combustion. Similarly, N_2O

emissions rise with increasing oxygen availability and reducing combustion temperatures.

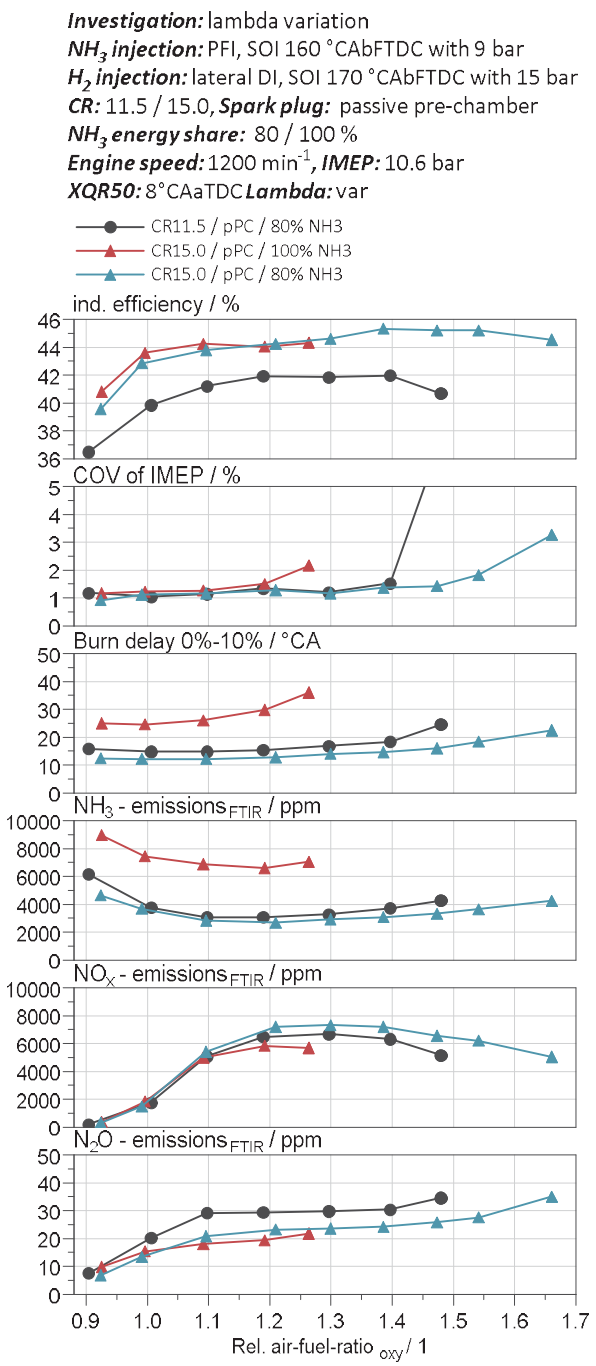

Figure 4 – Air-fuel-ratio variation

3.3 LOAD VARIATION

Figure 5 depicts a load variation at stoichiometric AFR operation with COC = 8° CA aTDC at 1200 1/min. Both the J-Gap spark plug and the passive pre-chamber were tested at 80% and 100% ammonia energy fraction with the CR = 15:1 setup. The CR = 11.5:1 tests with pure ammonia and the J-Gap spark plug as included for reference as well. The indicated efficiency shows a clear upwards trend with increasing load, again confirming that combustion is enhanced with elevated temperatures. The gap in efficiency between CR = 11.5 and CR = 15 is comparable to the NH_3 energy share variation shown in Figure 3.

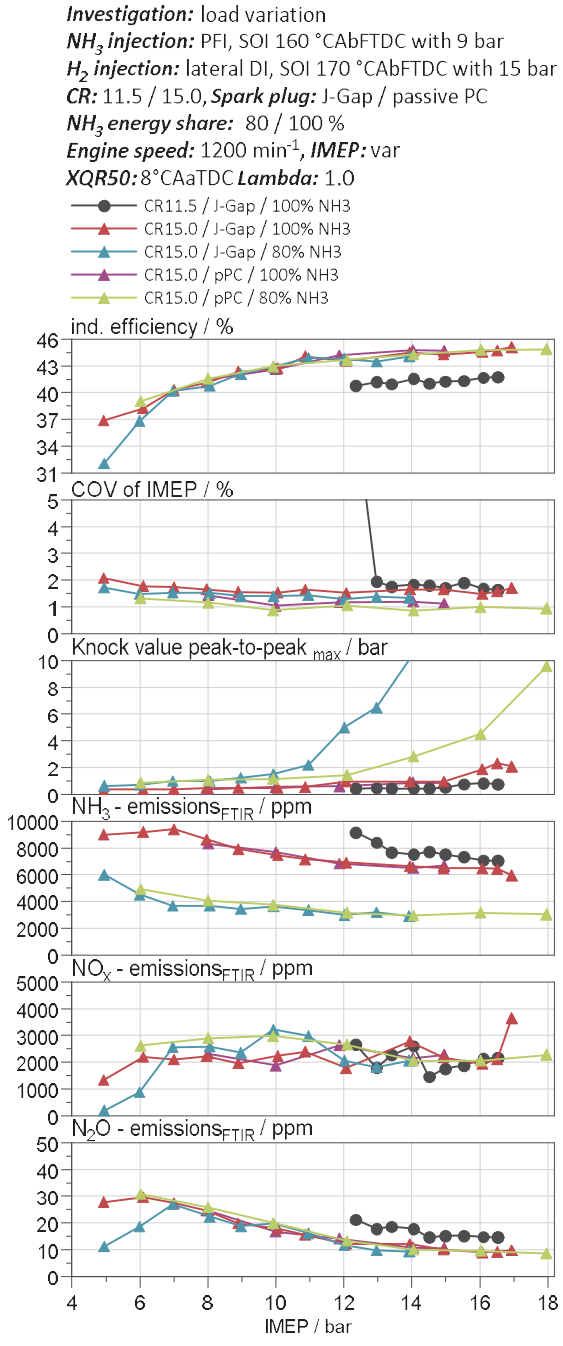

Figure 5 – Load variation

Spark knock is unfortunately observed for ammonia energy shares of 80%. The J-Gap spark plug configuration shows a knock onset at IMEP = 11 bar, while the prechamber spark plug shows first knocking at a relatively higher load of IMEP = 14 bar. This corresponds to a shorter

burn delay and a faster combustion with the passive prechamber. Load was limited mainly by the amount of ammonia that could be metered by the installed prototype injector.

As already evident from Figure 3, ammonia emissions are much lower with hydrogen blending. The trend of reducing NH_3 slip with increasing combustion temperatures is evident here as well.

For the NO_x emissions, no clear trend over the engine load is observed. Only for CR = 15 with 80% ammonia share a slight reduction with increasing load could be assumed. However, nitric oxide emissions at a rel. AFR = 1 are very sensitive to minor changes in the rel. AFR and the corresponding results should, therefore, not be overestimated.

Finally, the reduction in N_2O emissions with increasing load confirms the trend of reducing N_2O emissions with increasing temperatures observed beforehand in the other variations.

3.4 ENGINE MAP

To conclude the experimental section, selected parameters are shown in the investigated engine map. The configuration with passive pre-chamber and CR = 15:1 is exemplarily selected here, operated with an ammonia energy share of 80%. The results are depicted in Figure 6.

In this configuration, both the ammonia slip and NO_x emissions remain moderate with peak values in the range of 11 g/kWh. Since the ammonia to NO_x ratio is typically equal to 1 or slightly above, an SCR could be used for aftertreatment.

Indicated efficiency peaks above 45% represent a respectable value for an engine of this size and featuring just a pre-optimized combustion system definition. The combustion behavior is very stable with the COV of IMEP being close to 1% for almost all operating points. Knock onset is observed only from IMEP = 16 bar onwards for the fixed COC = 8° CA aTDC. Hence, with retarded spark timing, much higher loads or higher compression ratios would be probably possible

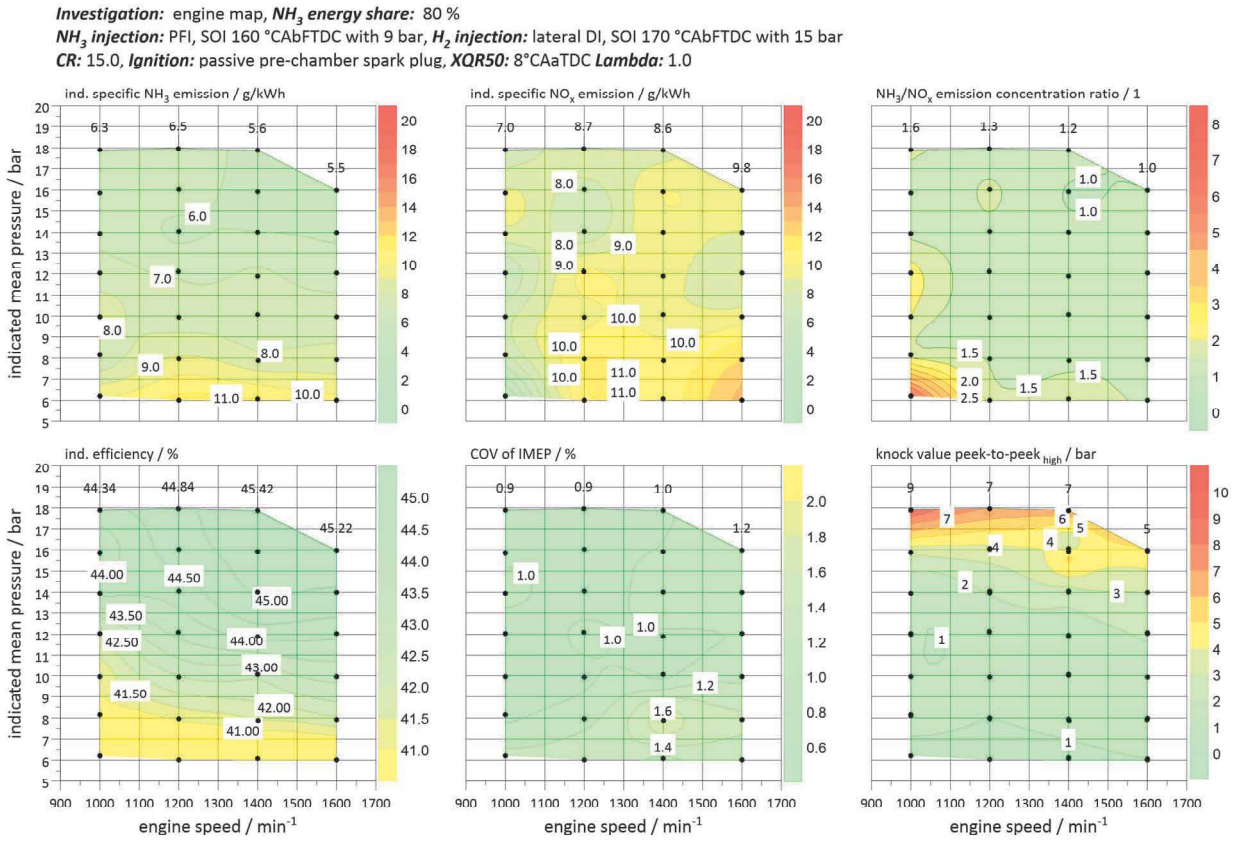

Figure 6 – Engine map for NH_3 energy share 80 %

To put the results into a complete perspective, Figure 7 depicts a comparison of key figures with different fuels in various combustion modes. While NO_x emissions are on a rather high level comparable to diesel combustion, aftertreatment with an SCR or three-way catalyst is possible without feeding further ammonia. As both NH_3 and H_2 are carbon free, the lowest CO_2 emissions are observed. The ammonia results plotted here include already the N_2O based GWP as CO_2 equivalent emissions

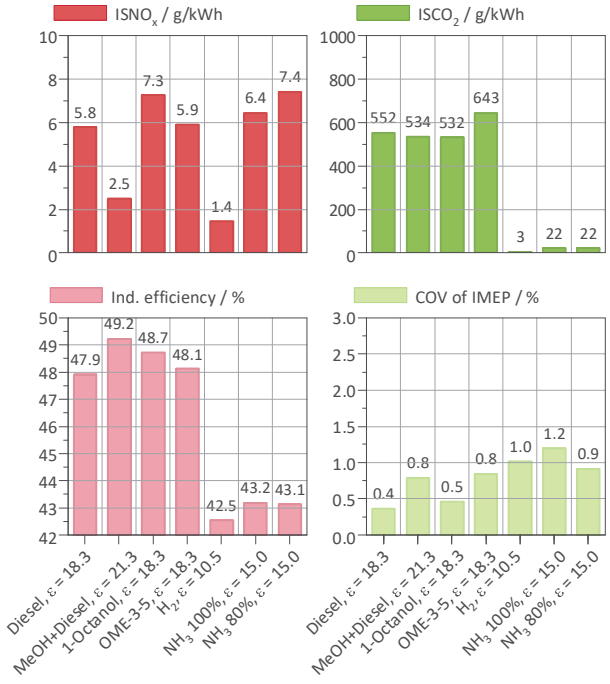

Figure 7 – Comparison of different fuels on FEV's single cylinder engine at IMEP = 10.6 bar and 1200 1/min

The indicated efficiency shows the highest values for diffusive methanol combustion as it also features the highest CR. Even with the drawbacks regarding combustion speed elaborated in the previous sections, due to its suitability for higher compression ratios, ammonia combustion yields a higher indicated efficiency than hydrogen combustion (with lower CR) – the only fuel in this overview combusted with positive ignition. Hence, both NH_3-H_2 blends as well as pure NH_3 combustion yield major potential for decarbonization of the power sector.

4 NUMERICAL INVESTIGATIONS

3D CFD simulations are used throughout the project for the analysis and visualizations of the obtained test bench measurements. As a first step, the ammonia investigations are used to calibrate the base CFD model. In the second step, the calibrated model is thoroughly extrapolated to simulate a large bore marine engine.

4.1 CALIBRATION OF CFD MODEL

The model of the engine (see Figure 1) used for the ammonia investigations is built up in 3D CFD code provided by Converge [11]. The solver version 3.0 is used for the simulations. The base grid size is 2.8 mm with the smallest cell size after refinement being 0.35 mm. The maximum number of cells in the domain is 2.5x10^5. Fluids are modeled as real gases, and the k-epsilon turbulence model is employed. Furthermore, the 3D gas exchange and injection processes are simulated to capture the mixture formation of the port fuel injection for 100% ammonia as well as for the operation with 20% hydrogen energy share.

Owing to the external mixture formation, the homogeneity in the combustion chamber at TDC is quite excellent as seen in Figure 8. The relative standard deviation of lambda ($\sigma_\lambda/\bar{\lambda}$) can be used to quantify the homogeneity, where lower values are better. For the pure NH_3 case this value is 5.9 %, which is considered as highly homogeneous.

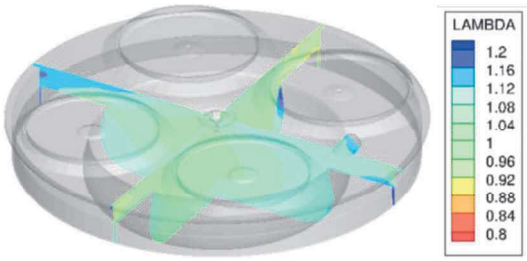

Figure 8 – Mixture distribution at 20°CA BTDC with 100% NH_3 operation

For the part substitution of ammonia with hydrogen, the latter is injected directly into the combustion chamber after IVC (Figure 9). Consequently, there is less time for mixture formation and the homogeneity of the mixture at TDC is reduced as reflected in the rel. standard deviation ($\sigma_\lambda/\bar{\lambda}$ = 13.5%) as seen in Figure 10.

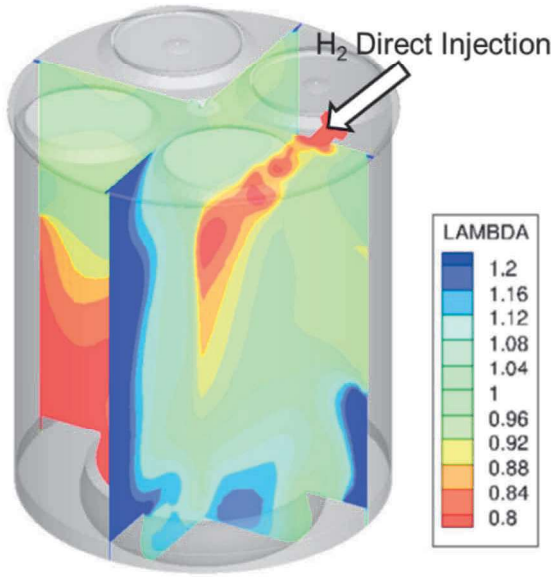

Figure 9 – Mixture distribution at 140°CA BTDC, 30°CA after H2 SOI with 80% NH_3 operation

Relative standard deviation of lambda ($\sigma_\lambda/\bar{\lambda}$) = 13.5 %

Figure 10 – Mixture distribution at 20°CA BTDC with 80% NH_3 operation

Detailed chemistry with the SAGE solver is used to model the combustion. The NH_3 combustion mechanism used for the calibration includes 32 species and 213 reactions [12]. The result of the calibration for a representative point with 100% ammonia is displayed in Figure 11.

The results confirm that the premixed flame propagation with NH_3 is reasonably captured by the calibrated combustion model after several iterations. Further calibration of the model with other operating points, ammonia shares and hydrogen blends for various spark timing sweeps is currently ongoing.

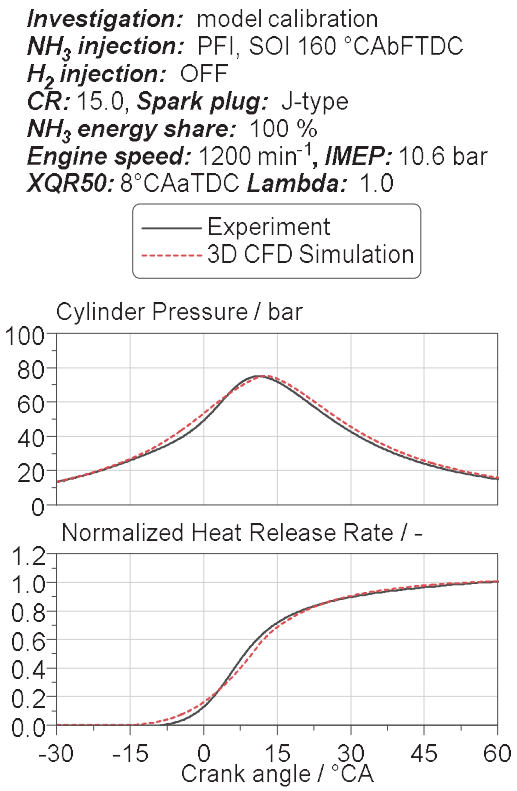

Figure 11 – Results of combustion model calibration

4.2 SIMULATION OF LARGE BORE MARINE ENGINE

In order to extend the findings from the FEV SCE to the commercial marine sector, where NH_3 is expected to play a significant role in decarbonization, an associated simulative study has been conducted. The bore size of the simulated engine geometry is set as 180 mm, while the stroke is chosen 220 mm (resulting in a ~5L cylinder displacement), which is representative for an industrial marine engine. The compression ratio is set to 17.5. The operating point selected for the in-detail simulations is 200 kW/cyl at 1500 1/min. The overall air-fuel-ratio is 1.87.

The substantially larger combustion chamber geometry poses challenges for premixed combustion, as the longer burn distances struggle to achieve reasonable burn durations. In extreme cases, it can promote knocking combustion, which requires a reduction of compression ratio and a penalty on the thermal efficiency, meaning increased fuel consumption for the targeted applications. To counteract this, a diesel pilot ignition has been applied to increase the range of the volumetric ignition while maximizing the ignition energy. Once ignited by the pilot fuel, the ammonia burns in a pre-mixed mode like the earlier experimental investigations. A higher ignition

energy by the diesel pilot can also help reduce the unburnt NH_3 emissions.

Consequently, the base model was adapted to the new engine geometry, dual-fuel mode and the new operating point. The diesel droplet breakup is modeled with the KH-RT model. Detailed chemistry is employed [13]. The mechanism is calibrated to data from [14]. The mechanism includes 69 species and 389 reactions. Ignition and combustion are handled with the SAGE model and the simulation is performed in one sector of the combustion chamber.

An ammonia energy share (AES) variation with diesel ignition and ammonia port injection is depicted in Figure 12 and Figure 13. The study was started with pure diesel i.e. 0 % AES as a reference case and the AES was continuously varied to reach 90 % with 10% diesel energy share (DES), which corresponds to a nearly premixed combustion of NH_3 after the injection of the diesel pilot quantity. For this exemplary variation, the diesel injection timing is kept constant at 6° CA BTDC over the variation. For ammonia energy shares of 20% (DES80-AES20) and 40% (DES40-AES60), the ammonia background mixture is so lean that the NH_3 is mainly burned passively in the air that is consumed by the diesel flame. Heat release falls off earlier corresponding to the overall shorter diesel injection while the shape of the heat release remains mostly the same. This can also be seen in the OH mass fraction figures and the temperature plots.

Once the ammonia energy share approaches a level of 80% or above, the OH mass fraction extends also beyond the area typically entrained by the diesel flame. A clear premixed flame can be seen by the temperature distribution for DES20-AES80. Here, the heat release shows a sharp premixed peak corresponding to the diesel injection igniting the premixed ammonia charge that is then contributing significantly to the heat release rate. The richer the background mixture is while the diesel injection is still providing sufficient energy to ignite it, the faster the overall heat release becomes. While the indicated efficiency overall decreases with increasing AES, it increases for shares around 80% locally due to the best compromise between the combustion properties of the premixed mixture and the energy provided by the diesel injection.

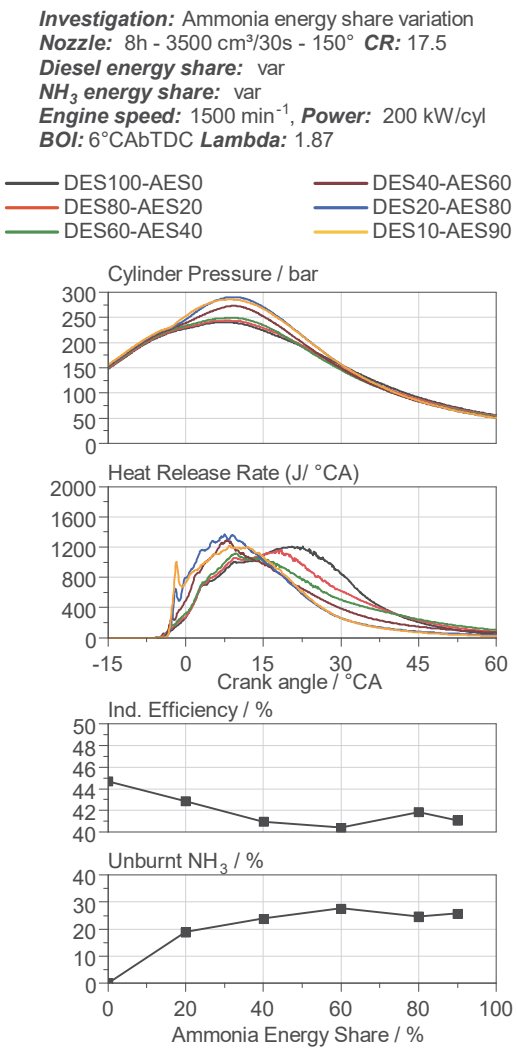

Figure 12 – Ammonia share variation with diesel dual fuel combustion

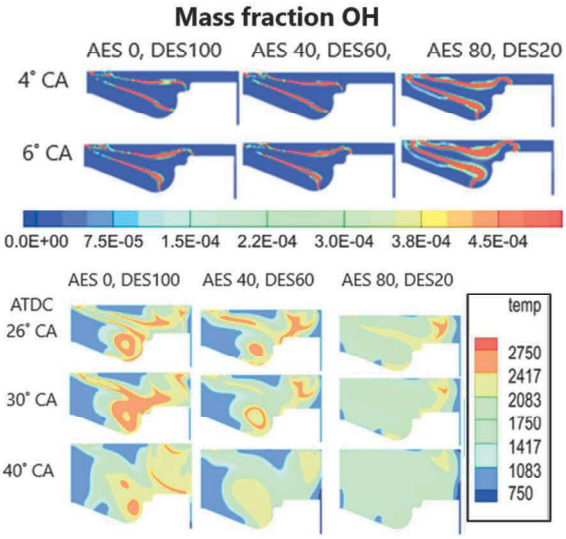

Figure 13 – Ammonia share variation with diesel dual fuel combustion – Cut sections

Identifying the necessity of richer NH_3 premixtures, a lambda variation (Figure 14 and Figure 15) was carried out with AES80-DES20. A lower lambda improves the combustion speed, unburnt NH_3 emissions and the efficiency at the cost of higher soot emissions. NO_x emissions are also reduced slightly.

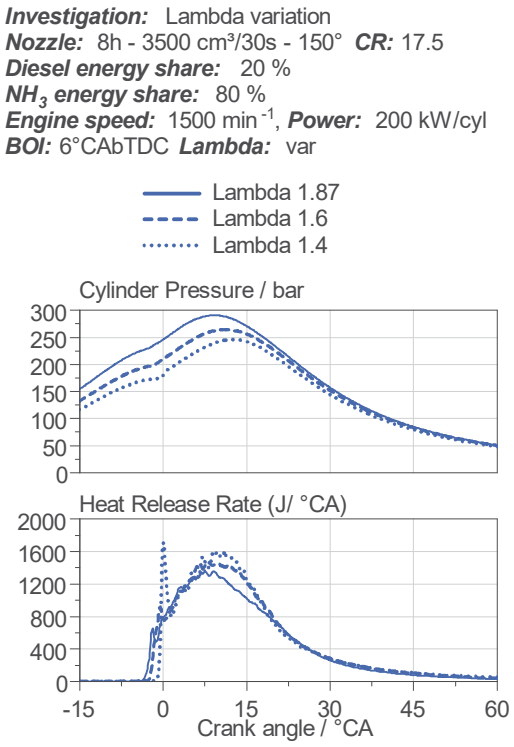

Figure 14 – Lamda variation with ammonia-diesel dual fuel combustion: pressure and HRR

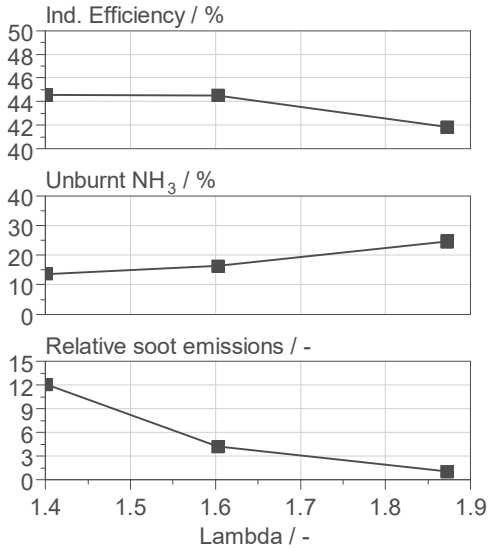

Figure 15 – Lamda variation with ammonia-diesel dual fuel combustion: efficiency and emissions

Furthermore, to increase the efficiency, hydrogen can be introduced into the combustion chamber with DES of 10%. This would necessitate a lowering of the CR to 13.5:1 and increasing the air-fuel ratio with increasing hydrogen energy share (HES) to avoid anomalous combustion. The results in Figure 16 display a faster combustion with increasing H_2 shares. This along with diminishing unburnt NH_3 increases the efficiency of the newly configured combustion system (Figure 17).

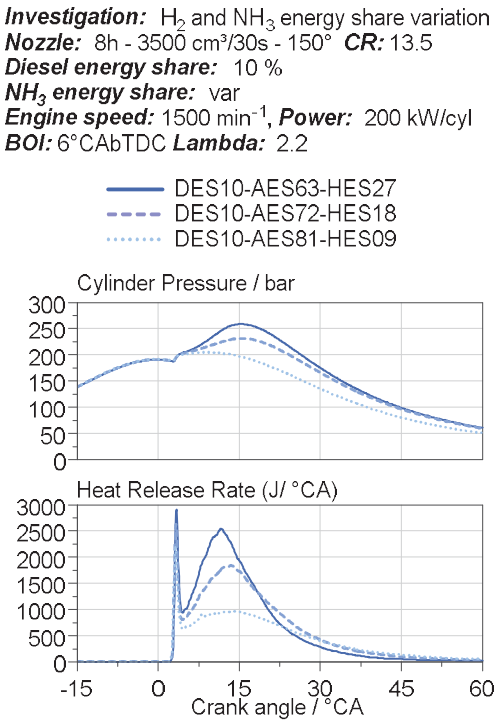

Figure 16 – Hydrogen energy share (HES) variation with ammonia-diesel dual fuel combustion: pressure and HRR

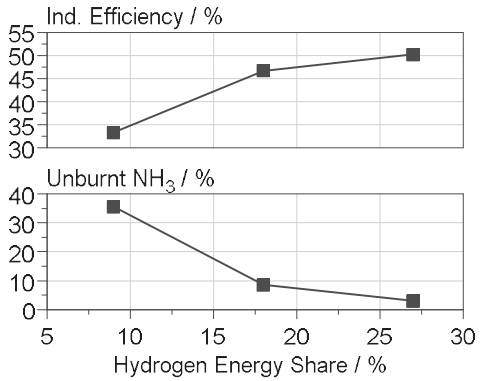

Figure 17 – Hydrogen energy share (HES) variation with ammonia-diesel dual fuel combustion: efficiency and emissions

These investigations help determine the influence of various hardware and operating parameters on the engine operation. These concept simulations

help guide the direction of optimization for the definition of the thermodynamic layout of such diesel-ammonia dual fuel engines.

5 SUMMARY AND CONCLUSIONS

Decarbonization is crucial for reducing GHG emissions and combating global warming. The future of carbon-free power generation relies on renewable and low-carbon energy carriers to meet rising energy demands while minimizing environmental impacts. The EU's FuelEU Maritime Initiative aims to promote sustainable marine fuels and zero-emission technologies, with H_2 and NH_3 being identified as key energy carriers for decarbonization.

Despite its relatively high energy density and established infrastructure, ammonia faces combustion challenges such as high ignition temperature, slow propagation and fuel-NO_x formation. Current research focuses on dual-fuel strategies using hydrogen to enhance ammonia's reactivity. A case study on FEV's adapted single cylinder research engine explores various ignition methods and modifications, highlighting the potential of hydrogen-ammonia combustion for stationary power generation and marine applications.

The experiments have been performed by varying ammonia shares, engine load and air fuel ratio. The results have been used to train and calibrate a CFD toolchain that was used to simulate the performance on a high-speed large bore engine with diesel ignition and ammonia port injection.

Results of the experimental investigation could be summarized as follows:

- The indicated efficiency of the combustion of pure ammonia is higher with a compression ratio (CR) of 15:1 compared to 11.5:1. Higher temperatures at CR = 15 improve ammonia ignitability. Addition of hydrogen shows better ignitability and faster burn durations. The hydrogen energy share is limited to 20% at CR = 15 due to pre-ignition, while conventional knock occurs at 50% hydrogen energy fraction at CR = 11.5.

- The coefficient of variation (COV) of IMEP increases sharply for J-Gap spark plugs and pre-chamber spark plugs at high ammonia shares for CR = 11.5, indicating low ignitability of ammonia with low CR.

- Ammonia emissions are high at low loads but decrease with increasing hydrogen content. Higher compression ratios reduce ammonia emissions due to elevated combustion chamber temperatures. Nitrogen oxide emissions are comparable to gasoline combustion in stoichiometric conditions and decrease with higher ammonia shares, while N_2O emissions rise with increasing ammonia share, showing a reduction at higher temperatures.

- A comparison of engine testing with different combustion systems and fuels was also presented. The indicated efficiency showed the highest values for diffusive methanol combustion. However, ammonia combustion yields a higher indicated efficiency than hydrogen combustion – the only fuel in the comparison combusted with positive ignition.

- CFD mixture formation simulations highlight the inhomogeneity with hydrogen direct injection as compared to pure ammonia port injection. The results of the SCE test bench are used to calibrate the CFD combustion model with detailed chemistry.

- As an outlook, the CFD model is used to simulate a large bore engine. The results indicate that the dual-fuel combustion with premixed ammonia and diesel pilot is a viable option and up to 90 % ammonia energy share can be achieved. To improve the efficiency and reduce unburnt NH_3, the air-fuel ratio can be lowered as long as the soot emissions are kept in check. Addition of hydrogen can further improve the flame propagation and combustion efficiency.

In conclusion, both ammonia-hydrogen blends and pure ammonia combustion offer significant potential for decarbonizing the power sector whereas diesel ammonia dual fuel combustion setups offer a viable option for large bore marine engines.

6 ACKNOWLEDGEMENTS

The author wishes to thank all the FEV colleagues who were involved in the development of this paper. The author would also like to thank Champion Ignition for providing the advanced ignition system.

7 REFERENCES AND BIBLIOGRAPHY

[1] Indlekofer, Haugen, Forde, Gruber, SINTEF Energy Research, Norwegian University of Science and Technology, Department of Energy and Process Engineering, Numerical Investigation of Premixed and Non-premixed Ammonia Main Charge Configurations Ignited by a Hydrogen-Fired Prechamber

[2] Mounaïm-Rousselle, Bréquigny, Dumand, Houillé; Energies 14, 2021: Operating limits for ammonia fuel spark-ignition engine

[3] Lhuillier, Brequigny, Contino, Mounaïm-Rousselle, Fuel Vol. 269, 2020: Experimental study on ammonia/hydrogen/air combustion in spark ignition engine conditions

[4] REGULATION (EU) 2023/1805 OF THE EUROPEAN PARLIAMENT AND OF THE COUNCIL of 13 September 2023 on the use of renewable and low-carbon fuels in maritime transport, and amending Directive 2009/16/EC

[5] Weltenergierat Deutschland, 2023: Ammoniak als Energieträger für die Energiewende

[6] Valera-Medina, Xiao, Owen-Jones, David, Bowen; Progress in Energy and Combustion Science 69, 2018: Ammonia for Power

[7] Stefanova, Chuturkova; GSTF Journal of Engineering Technlogy 3, 2015: Technical Engineering for Catalytic Reduction of Nitrous Oxide Emissions

[8] Güdden, Franzke, Boberic, Zimmer, Pischinger; 13th Dessau Gas Engine Conference, May 2024; Performance improvement of direct injection H2-ICE with flat cylinder heads

[9] Güdden, Pischinger, Geiger, Heuser, Müther; 18th Symposium „Sustainable Mobility, Transport and Power Generation", September 2021; Methanol Combustion Systems for Heavy-Duty Applications: Diffusive or Premixed Combustion?

[10] Kobayashi, Hayakawa, Kunkuma, Somarathne, Okafor; Proceedings of the Combustion Institute 23, 2019: Science and technology of ammonia combustion

[11] Converge User Manual 3.0, Convergent Science, 2020.

[12] Otomo, Junichiro, et al. "Chemical kinetic modeling of ammonia oxidation with improved reaction mechanism for ammonia/air and ammonia/hydrogen/air combustion." *International Journal of Hydrogen Energy* 43.5 (2018): 3004-3014.

[13] Xu, Chang, Treacy, Zhou, Jia, Bai; 2023; A skeletal chemical kinetic mechanism for ammonia

[14] Yu, Zhou, Feng, Wang, Zhu, Qian, Lu; 2020; The effect of ammonia addition on the low-temperature autoignition of n-heptane: an experimental and modeling study; Combustion and Flame, 217, pp.4-11